Since January 2020 Elsevier has created a COVID-19 resource centre with free information in English and Mandarin on the novel coronavirus COVID-19. The COVID-19 resource centre is hosted on Elsevier Connect, the company's public news and information website.

Elsevier hereby grants permission to make all its COVID-19-related research that is available on the COVID-19 resource centre - including this research content - immediately available in PubMed Central and other publicly funded repositories, such as the WHO COVID database with rights for unrestricted research re-use and analyses in any form or by any means with acknowledgement of the original source. These permissions are granted for free by Elsevier for as long as the COVID-19 resource centre remains active.

Veterinary Microbiology 213 (2018) 114–122

Contents lists available at ScienceDirect

Veterinary Microbiology

journal homepage: www.elsevier.com/locate/vetmic

Identification of two antiviral inhibitors targeting 3C-like serine/3C-like protease of porcine reproductive and respiratory syndrome virus and porcine epidemic diarrhea virus

Yuejun Shi[a,b,c,d], Yingying Lei[a,b], Gang Ye[a,b,c], Limeng Sun[a,b,c], Liurong Fang[a,b,c], Shaobo Xiao[a,b,c], Zhen F. Fu[a,b,c,f], Ping Yin[d,e], Yunfeng Song[a,b,c,*], Guiqing Peng[a,b,c,*]

[a] State Key Laboratory of Agricultural Microbiology, Huazhong Agricultural University, Wuhan 430070, China
[b] College of Veterinary Medicine, Huazhong Agricultural University, Wuhan 430070, China
[c] The Cooperative Innovation Center for Sustainable Pig Production, Huazhong Agricultural University, Wuhan 430070, China
[d] College of Life Science and Technology, Huazhong Agricultural University, Wuhan 430070, China
[e] National Key Laboratory of Crop Genetic Improvement and National Centre of Plant Gene Research, Huazhong Agricultural University, Wuhan 430070, China
[f] Departments of Pathology, College of Veterinary Medicine, University of Georgia, Athens, GA 30602, USA

ARTICLE INFO

Keywords:
PRRSV
PEDV
Antiviral inhibitor
Broad-spectrum
3C-like serine/3C-like protease

ABSTRACT

Porcine reproductive and respiratory syndrome virus (PRRSV) and porcine epidemic diarrhea virus (PEDV) are highly virulent and contagious porcine pathogens that cause tremendous economic losses to the swine industry worldwide. Currently, there is no effective treatment for PRRSV and PEDV, and commercial vaccines do not induce sterilizing immunity. In this study, we screened a library of 1000 compounds and identified two specific inhibitors, designated compounds 2 and 3, which target the PRRSV 3C-like serine protease (3CLSP). First, we evaluated the inhibitory effects of compounds 2 and 3 on PRRSV 3CLSP activity. Next, we determined the anti-PRRSV capacity of compounds 2 and 3 in MARC-145 cells and obtained EC_{50} and CC_{50} values of 57 μM (CC_{50} = 479.9 μM) and 56.8 μM (CC_{50} = 482.8 μM), respectively. Importantly, compounds 2 and 3 also targeted the PEDV 3C-like protease (3CL protease) and inhibited PEDV replication, showing EC_{50} and CC_{50} values of 100 μM (CC_{50} = 533.8 μM) and 57.9 μM (CC_{50} = 522.3 μM), respectively. Finally, our results indicated that the active sites (His39 in 3CLSP and His41 in 3CL protease) were conservative, and contacted compounds 2 and 3 via hydrogen bonds and hydrophobic forces in the putative substrate-binding models. In summary, compounds 2 and 3 exhibit broad-spectrum antiviral activity and may facilitate the development of antiviral drugs against PRRSV and PEDV.

1. Introduction

Nidoviruses are important pathogens of both humans and livestock; they are enveloped, plus-strand RNA viruses comprising the families *Arteriviridae* and *Coronaviridae* (Gorbalenya et al., 2006). Porcine reproductive and respiratory syndrome virus (PRRSV), a member of the family *Arteriviridae* (Snijder et al., 2013), has been a major threat to the worldwide swine industry since its discovery in the early 1990s (Wensvoort et al., 1991; Collins et al., 1992). In 2006, a highly pathogenic porcine reproductive and respiratory syndrome virus (HP-PRRSV) emerged and prevailed in mainland China, resulting in devastating damage to swine production (Tian et al., 2007). Currently, HP-PRRSV causes high morbidity and high mortality in infected pigs of all ages and has remained a major threat to the swine producers in China and surrounding countries (Han et al., 2017). Porcine epidemic diarrhea virus (PEDV), a member of the genus *Alpha-coronavirus* (Song and Park, 2012), was first identified in the 1980s in China (Xuan et al., 1984). PEDV causes a contagious intestinal disease called porcine epidemic diarrhea (PED), which is characterized by vomiting, diarrhea, and dehydration (Wang et al., 2016). In October 2010, a large-scale outbreak of PED caused by a PEDV variant occurred in China, resulting in tremendous economic losses (Li et al., 2012; Wang et al., 2013, 2016; Tian et al., 2014). PRRSV and PEDV are highly virulent and contagious porcine pathogens that cause respiratory and enteric disease in pigs and result in significant economic losses for the intensive pig production worldwide (Li et al., 2012; Snijder et al., 2013; Wang et al., 2016).

* Corresponding authors at: State Key Laboratory of Agricultural Microbiology, College of Veterinary Medicine, Huazhong Agricultural University, 1 Shi-zi-shan Street, Wuhan 430070, China.
E-mail addresses: syf@mail.hzau.edu.cn (Y. Song), penggq@mail.hzau.edu.cn (G. Peng).

https://doi.org/10.1016/j.vetmic.2017.11.031
Received 29 September 2017; Received in revised form 20 November 2017; Accepted 23 November 2017
0378-1135/ © 2017 Elsevier B.V. All rights reserved.

In the PRRSV and PEDV genome, ORF1a and ORF1b comprise approximately 80% of the genome and encode polyproteins (pp1a and pp1b) that are cleaved by viral proteases into intermediate and mature nonstructural proteins (Ziebuhr et al., 2000; Gorbalenya et al., 2006). The viral proteases involved in polyprotein cleavage are papain-like proteases (PL1pro and PL2pro) and a 3CL serine protease (PRRSV nsp4; 3CLSP)/3C-like (PEDV nsp5; 3CL) protease (Tian et al., 2009; Ye et al., 2016). During replication, the PL1pro and PL2pro proteases cleave the N-proximal region of pp1a/pp1ab, and the 3CLSP/3CL protease cleaves the viral polyprotein at other conserved inter-domain junctions (Tian et al., 2009; Ye et al., 2016). The viral 3CLSP/3CL proteases play an essential role in *artertivirus* and *coronavirus* replication; therefore, they have received much attention as potential key antiviral targets (including TGEV, FIPV, IBV and SARS-CoV) (Anand et al., 2002; Kim et al., 2013; Lee et al., 2007; Xue et al., 2008).

As RNA viruses, PRRSV and PEDV are prone to mutation under selective pressures in the field, and this may cause the frequent appearances of new variant strains (Wang et al., 2016; Han et al., 2017). Moreover, current commercial vaccination approaches against PRRSV and PEDV are only partially effective (Wang et al., 2016; Du et al., 2017a,b). To date, effective broad-spectrum antiviral drugs for PRRSV and PEDV infections are not available, although antiviral compounds have been reported previously (Karuppannan et al., 2012; St John et al., 2016; Evans et al., 2017). This remains an impediment to identifying new inhibitors that target the PRRSV and PEDV 3CLSP/3CL proteases for use as antiviral therapies during disease epidemics. In this study, our findings provide new insights into the molecular mechanisms underlying 3CLSP or 3CL protease-mediated inhibition of viral replication and may also guide the development of new broad-spectrum antiviral drugs.

2. Materials and methods

2.1. Compounds

A low-molecular-weight fragment-based library containing approximately 1000 compounds (Specs, Delf, Netherlands) was used for antiviral fragment screening. These fragments are defined as small molecules obeying the Congreve 'Rule of three' in which molecular weight (MW) ≤ 300, the number of hydrogen donors and acceptors ≤ 3 and cLogP ≤ 3 (Congreve et al., 2003). All these compounds were dissolved in dimethyl sulfoxide (DMSO; Mpbio) at a concentration of 10 mM. Moreover, compounds 1–5 were prepared in DMSO as stock solutions (50 mM).

2.2. Viruses and cells

Marc-145 cells (a PRRSV-permissive cell line derived from MA-104 cells) (Kim et al., 1993) and African green monkey cells (Vero cells; Cat. No. CCL-81) were cultured in Dulbecco's minimum essential medium (DMEM, HyClone), supplemented with 10% fetal bovine serum (Gibco) at 37 °C with 5% CO_2. Moreover, the HP-PRRSV WUH3 strain (GenBank accession no. HM853673) (Li et al., 2009) and the PEDV FJZZ strain (GenBank: KC140102.1) were used in all assays.

2.3. Expression and purification of PRRSV nsp4 (3CLSP) and PEDV nsp5 (3CL protease)

For expression of PRRSV 3CLSP, the coding sequence was PCR-amplified from the PRRSV WUH3 strain cDNA library and inserted into pET-42b (+) with a C-terminal His_6-tag at the *NdeI* and *BamHI* restriction sites. All constructs were validated by DNA sequencing. The plasmid was transformed into *Escherichia coli* strain BL21(DE3), and cells were cultured at 37 °C in LB medium containing 50 mg/l kanamycin. When the optical density at 600-nm (OD_{600}) reached 0.8, the culture was cooled to 18 °C and supplemented with 0.8 mM IPTG (isopropyl–D-thiogalactopyranoside). After overnight induction, the cells were harvested via centrifugation at 8500 rpm (30 min, 4 °C). Protein purification followed our previously reported procedure (Shi et al., 2016). Finally, the harvested protein was concentrated to a volume of approximately 2.0 ml and filtered using a Superdex 200 gel filtration column (GE Healthcare) equilibrated with buffer (20 mM Tris–HCl and 200 mM NaCl, pH 7.4). The concentration of the purified protein was determined by detecting the absorbance at 280-nm (A280) using a NanoDrop 2000c UV–vis spectrophotometer (Thermo Fisher Scientific). PEDV 3CL protease expression and purification were carried out following our previously reported procedure (Ye et al., 2016).

2.4. Measurement of IC_{50}

The polypeptide substrate Dabsyl-KTAYFQLE↓GRHFE-Edans (Tian et al., 2009) and Dabcyl-YNSTLQ↓AGLRKM-E-Edans (Ye et al., 2016) were chemically synthesized by the GenScript Corporation. PRRSV 3CLSP and PEDV 3CL proteases were used at a final concentration of 2 μM and 0.25 μM, respectively. Compounds at various concentrations (6.25–500 μM) were pre-incubated with protease for 20 min at 37 °C, and 1 μM (3CLSP substrate) or 10 μM (3CL protease substrate) was added to the mixture in a black 96-well plate. The mixtures were then further incubated at 37 °C for 60 min, and enhanced fluorescence due to substrate cleavage by 3CLSP/3CL protease was monitored at 340 excitation and 485 emission. The relative fluorescence units (RFU) were calculated by subtracting the background (substrate control well without protease) from the fluorescence readings. The percentage of inhibition was calculated as follows: Percentage of inhibition (%) = 100 × [1 − RFU of the experimental group (60 min– 0 min)/RFU of the control group (60 min–0 min)].

2.5. Cell viability assay

The 50% cell death toxic concentrations (CC_{50}) of compounds 2, 3 and 5 in MARC-145 cells and Vero cells were determined following our previously reported procedure (Shi et al., 2016). Briefly, confluent cells grown in white 96-well plates (Corning, Tewksbury, MA, USA) were treated with various concentrations (50–500 μM) of compounds for 72 h. MARC-145 cells or Vero cells were treated with 0.1% DMSO as control. Cell cytotoxicity was measured using the Celltiter-Glo Luminescent Cell Viability Assay reagent (Promega, Madison, WI, USA).

2.6. $TCID_{50}$ assay for PRRSV and PEDV

MARC-145 cells were seeded in 12-well plates at a density of 2.5×10^5 cells per well. When cells were grown to 70–80% confluence, PRRSV was added with increasing concentrations of compounds 2, 3 and 5 (6.25 μM, 12.5 μM, 25 μM, 50 μM, 100 μM and 200 μM) at a multiplicity of infection (MOI) of 0.1, and then supernatants containing virus and compounds were used to infect MARC-145 cells for 36 h. Then, the harvested supernatant (include PRRSV and compounds) was used for $TCID_{50}$ assays. Briefly, MARC-145 cells were seeded in 96-well plates, and infected with serial 10-fold dilutions of supernatant using eight replicates in $TCID_{50}$ assays. The plates were incubated for 72–96 h before viral titers were calculated. The $TCID_{50}$ assay for PEDV was also performed following the same methods.

2.7. Western blot analysis

MARC-145 cells or Vero cells were seeded in 6-well plates at a density of 5×10^5–1×10^6 cells per well. When cells were grown to 70–80% confluence, the PRRSV WUH3 strain and the PEDV FJZZ strain were inoculated into cells at an MOI of 0.1. Virus-infected cells were incubated in the presence of compounds (6.25 μM, 12.5 μM, 25 μM, 50 μM, 100 μM and 200 μM) for up to 36 h. Then, compound-treated PRRSV/PEDV-infected or control cells (0.4% DMSO) were lysed in a

lysis buffer (20 mM Tris [pH 7.5], 150 mM NaCl, 1% Triton X-100) containing proteinase inhibitors (Beyotime). Supernatants were harvested, and the total protein for each sample was measured using a BCA protein assay kit (Thermo Scientific). Equal amounts of protein for each sample were analyzed by performing 12% SDS-PAGE followed by transfer to PVDF membranes (Bio-Rad). After blocking, the membranes were incubated overnight at 4 °C with an anti-PRRSV/PEDV nucleocapsid (N) protein monoclonal antibody (1:3000) and an anti-GAPDH monoclonal antibody (1:5000; Proteintech). Finally, the membranes were incubated with goat-anti-mouse secondary antibody (Boster Biological Technology Co., Ltd.) for 1 h (1:5000). Then, the membranes were visualized using an enhanced chemiluminescence system (Amersham Imager 600, GE Healthcare). Densitometry analysis of the levels of nucleocapsid protein levels have been measured by Image J software, and normalized to GAPDH.

2.8. In silico docking

The crystal structures of PRRSV nsp4 (3CLSP, PDB: 5Y4L) and PEDV nsp5 (3CL protease, PDB: 4XFQ) and the complex structure of PEDV nsp5 (3CL protease, PDB: 4ZUH) were retrieved. Homology models of PRRSV nsp4 and PEDV nsp5 with compounds 2 and 3 were generated using Autodock 4 software. The root mean square deviation (RMSD) and the most likely binding pattern were analyzed using PDBeFold (http://pdbe.org/fold/) and PyMOL (Schrödinger), respectively. The amino acid sequences of *Arterivirus* (PRRSV and EAV) 3CLSP and PEDV 3CL protease were aligned using ClustalW2 (Larkin et al., 2007) and visualized with the ESPript 3.0 server (http://espript.ibcp.fr) (Robert and Gouet, 2014).

2.9. Statistical analysis

IC_{50}, CC_{50} and EC_{50} were determined using GraphPad Prism software 5 (GraphPad Software, San Diego, CA). All experiments were performed in triplicate, and values (± standard deviations [SD]) are shown. Significant differences were determined using Student's *t*-test. *, $P < 0.05$ (considered significant compared with control group); **, $P < 0.01$ (considered highly significant); ***, $P < 0.001$ (considered extremely significant).

3. Results

3.1. Identification of inhibitors that target PRRSV nsp4 (3CLSP)

A library of 1000 lead compounds was screened against PRRSV 3CLSP using FRET assays. Preliminary screening was done at 2 μM PRRSV nsp4, 1 μM substrate and 200 μM compounds. Five compounds inhibiting more than 70% of the protease activity under these conditions were selected for further IC_{50} measurements (Fig. 1A). These compounds, designated compounds 1–5, are shown in Fig. 1B; their Specs ID numbers are AQ-405/42656504, AE-562/12222651, AE-562/12222652, AC-907/34117033 and AF-399/13804049, respectively (Table 1). Other detailed information is shown in Table S1.

To evaluate their inhibitory effects on 3CLSP activity, we added different concentrations (50 μM, 100 μM, 200 μM, 300 μM, 400 μM and 500 μM) of compounds 1–5 to the protease reaction mixture, and the percentage of inhibition was calculated based on the observed fluorescence. All compounds showed concentration-dependent inhibition, with inhibition levels reaching as high as 60–80% (Fig. 2A–E). The IC_{50} values, estimated by non-linear regression, were 202.3 μM (compound 1), 144.3 μM (compound 2), 115.9 μM (compound 3), 147.8 μM (compound 4) and 172.9 μM (compound 5). Meanwhile, the effects of DMSO on 3CSLP activity were also determined (Fig. S1). Interestingly, 3CSLP activity exhibited a concentration-dependent trend along with increased DMSO concentration (1–10%), which may lead to the high IC_{50} values.

3.2. Suppression of PRRSV replication by compounds 2, 3 and 5

To evaluate the suppression of PRRSV replication by compounds 2, 3 and 5, we added each compound to PRRSV-infected cells over a range of concentrations (6.25 μM, 12.5 μM, 25 μM, 50 μM, 100 μM and 200 μM). The EC_{50} values of compounds 2, 3 and 5 were estimated at 57 μM, 56.8 μM and 200 μM, respectively (Fig. 3B). Furthermore, all three compounds showed low cytotoxicity. The CC_{50} values of compounds 2 and 3 were estimated at 479.9 μM and 482.8 μM (Fig. 3A), respectively, whereas cell viability was higher than 60% in the presence of compound 5 at 500 μM (Fig. 3A). Although significant cytotoxicity was observed at concentrations higher than 200 μM, compounds 2 and 3 strongly inhibited PRRSV infection at 100 μM (Fig. 3A and B). Hence, our results showed that compounds 2 and 3 significantly inhibited PRRSV replication at non-cytotoxic concentrations (the S.I. values were approximately 8.42 and 8.5, respectively) (Table 1). Interestingly, we observed that the EC_{50} was higher than the IC_{50}, which may be due to the presence of a membrane barrier or the high protease concentration (1 μM) used in the FRET assay, as previously reported (Kumar et al., 2017).

To further quantify the inhibitory effects of compounds 1–5, we detected PRRSV nucleocapsid (N) protein expression by western blot (Fig. 3C). PRRSV N protein was decreased by compounds 2, 3 and 5 in a dose-dependent manner. Notably, no viral N protein was detectable in the presence of compounds 2 and 3 at 100 μM, which indicated that these compounds markedly inhibited PRRSV propagation in MARC-145 cells. Compounds 1 and 4 did not substantially suppress PRRSV replication (Fig. 3C); differences in their molecular structures may cause weak inhibitory effects on PRRSV replication.

3.3. The broad spectrum antiviral activity of compounds 2 and 3 extends to PEDV nsp5 (3CL protease)

PRRSV and PEDV belong to the order *Nidovirales* and possess similarities in genome organization and strategies for nonstructural and structural protein expression (Ziebuhr et al., 2000). Hence, we evaluated the inhibitory effects of compounds 2 and 3 on PEDV 3CL protease activity in the FRET assay. Both compounds showed concentration-dependent inhibition, with inhibition levels reaching as high as 80% (Fig. 4A). The IC_{50} values were 37.8 μM (compound 2) and 23.4 μM (compound 3), as estimated by non-linear regression. Meanwhile, the ability of compounds 2 and 3 to block PEDV replication was also evaluated. The PEDV strain was sensitive to both compounds with EC_{50} values of 100 μM and 57.9 μM, respectively (Fig. 4C), and PEDV N protein was decreased by compounds 2 and 3 in a dose-dependent manner (Fig. 4D). Furthermore, CC_{50} values measured in Vero cells were 533.8 μM and 522.3 μM (Fig. 4B), and the S.I. values were approximately 5.34 and 9.02 (Table 1), respectively. Additionally, our results showed that the protease activity of EAV 3CLSP was inhibited by compound 3 (Fig. S1). Therefore, compounds 2 and 3 behave as potential broad-spectrum antiviral agents.

3.4. Potential binding sites

The complex crystal structures of protein-compounds are used to guide the organic synthesis of high-affinity protein ligands and enzyme inhibitors (de Kloe et al., 2009). In this study, we soaked PRRSV 3CLSP and PEDV 3CL protease crystals with various concentrations of compounds 2 and 3. Unfortunately, we were unable to obtain complex structures. Therefore, the potential binding sites were analyzed in detail using molecular simulations to dock compounds 2 and 3 into the PRRSV 3CLSP and PEDV 3CL protease structures (Fig. 5A and B). The complex models were initially positioned based on the X-ray structures (Streptomyces griseus proteinase E, SGPE, PDB code: 1HPG; PEDV nsp5: 4ZUH) (Nienaber et al., 1993; Ye et al., 2016). Grid maps of 40 × 40 × 40 grid points, centered on the substrates of the complex

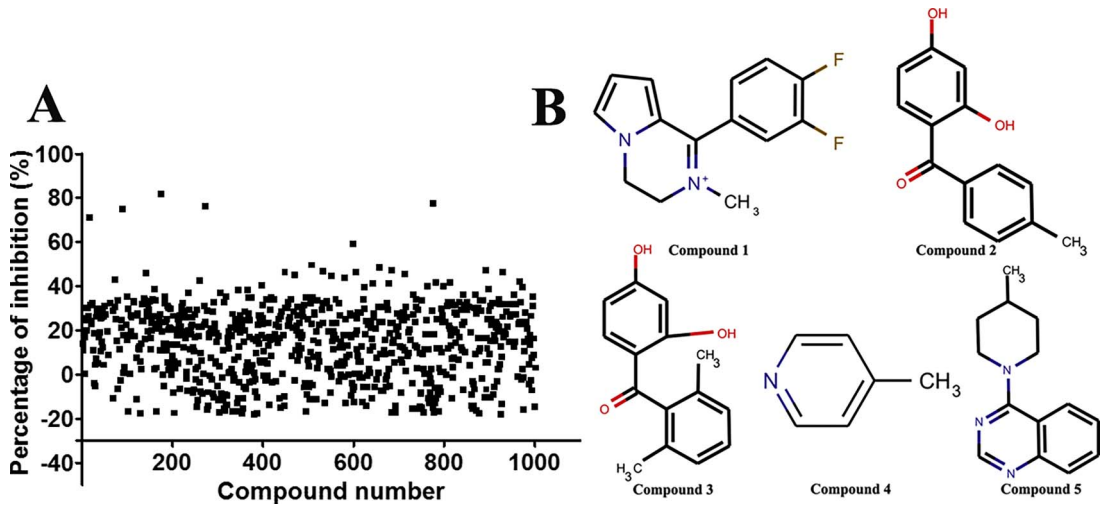

Fig. 1. Screening inhibitors targeting PRRSV 3CLSP from a low-molecular-weight fragment-based library. Each dot represents the percentage of inhibition from compounds at concentrations of 200 μM. (A) Five compounds exhibited inhibition levels greater than 70% and were designated compounds 1–5. (B) The two-dimensional structures of compounds 1–5.

structures, covered the binding pockets. A population size of 150, mutation rate of 0.02, and crossover rate of 0.8 were set as the parameters. Simulations were performed using up to 2.5 million energy evaluations with a maximum of 27,000 generations. Each simulation was performed 100 times, yielding 256 docked conformations. The lowest energy conformations were regarded as the binding conformations between the ligands and the proteins (Wei et al., 2008). In the complex models, compounds 2 and 3 interacted with 3CLSP/3CL proteases via extensive hydrogen bonds and hydrophobic forces (Fig. 5A and B).

The active sites of the PRRSV nsp4 consist of His39, Asp64 and Ser118; additionally, the S1 specificity pocket is conserved in *arteriviruses* (PRRSV and EAV) and comprises His133 and Ser136 (corresponding to His134 and His137 of EAV nsp4) (Fig. 5C) (Tian et al., 2009). Indeed, the active sites (His39, Asp64 and Ser118) and S1 specificity pocket (His133 and Ser136) of PRRSV nsp4 interacted with compounds 2 and 3 via hydrogen bonds and hydrophobic forces (Fig. 5A). In PEDV, the active sites of the nsp5 was composed of His41 and Cys144, and the S1 specificity pocket consists of Phe139, Ile140, Asn141, Gly142, Ala143, Cys144, His162, Gln163 and Glu165 (Ye et al., 2016). Analogously, extensive interactions among compounds 2, 3 and the active site (His41) and S1 specificity pocket (Glu165) of the PEDVnsp5 were also observed (Fig. 5B). Hence, compounds 2 and 3 may block the recognition and combination of the 3CLSP/3CL proteases and substrates, thereby inhibiting PRRSV and PEDV replication.

Multiple-sequence alignment indicated that the amino acid sequence identity between PRRSV nsp4 and PEDV nsp5 was approximately only 22.2% (Fig. 5C). Moreover, there were distinct differences between the structures of the 3CLSP and 3CL protease (RSMD is 2.66). Interestingly, the active site His39 in PRRSV nsp4 (corresponding to His41 of PEDV nsp5) is conservative (Fig. 5C). Meanwhile, these two sites contact compounds 2 and 3 via hydrogen bonds and hydrophobic forces (Fig. 5A and B), which may be the reason that compounds 2 and 3 exhibit broad-spectrum activity against PRRSV and PEDV.

4. Discussion

Porcine reproductive and respiratory syndrome virus (PRRSV) and porcine epidemic diarrhea virus (PEDV) are major threats to the worldwide swine industry. Currently, both inactivated and live attenuated virus vaccines have been used in the intensive pig farm. Although reducing mortality, the currently used vaccines cannot to control PRRSV and PEDV infection and spread. Furthermore, no commercial drugs are available to prevent their infection. For *Nidoviruses*, the 3CLSP and 3CL protease are key players in viral replication (Xue et al., 2008). Hence, the development of anti-viral drugs targeting the 3CLSP and 3CL proteases would become an important strategy for preventing PRRSV and PEDV outbreaks.

In our experiment, the compounds screening targeting 3CLSP and 3CL protease was used to identify inhibitors that suppress PRRSV and PEDV replication. Meanwhile, to elucidate the binding mechanism of compounds and 3CLSP or 3CL proteases, we simulated the most likely binding conformations using Autodock 4 software. In the 3CLSP and

Table 1
Antiviral activity of compounds against PRRSV and PEDV.

Compounds	Name	PRRSV-3CL^{pro}				PEDV-3CL^{pro}			
		IC_{50} (μM)	CC_{50}[a] (μM)	EC_{50} (μM)	SI[b] values	IC_{50} (μM)	CC_{50}[c] (μM)	EC_{50} (μM)	SI values
1	1-(3,4-difluorophenyl)-2-methyl-3,4-dihydropyrrolo[1,2-a] pyrazin-2-ium	202.3	ND	> 300	ND	ND	ND	ND	ND
2	(2,4-dihydroxyphenyl) (4-methylphenyl)methanone	144.3	479.9	57	8.42	37.8	533.8	100	5.34
3	(2,4-dihydroxyphenyl)(2,6-dimethylphenyl)methanone	115.9	482.8	56.8	8.5	23.4	522.3	57.9	9.02
4	4-methylpyridine	147.8	ND	> 300	ND	> 500	ND	ND	ND
5	4-(4-methylpiperidin-1-yl)quinazoline	172.9	738.1	200	3.69	ND	ND	ND	ND

ND: Not determined.
[a] 50% cytotoxic concentration in MARC-145 cells.
[b] selectivity index (SI) values.
[c] 50% cytotoxic concentration in Vero cells.

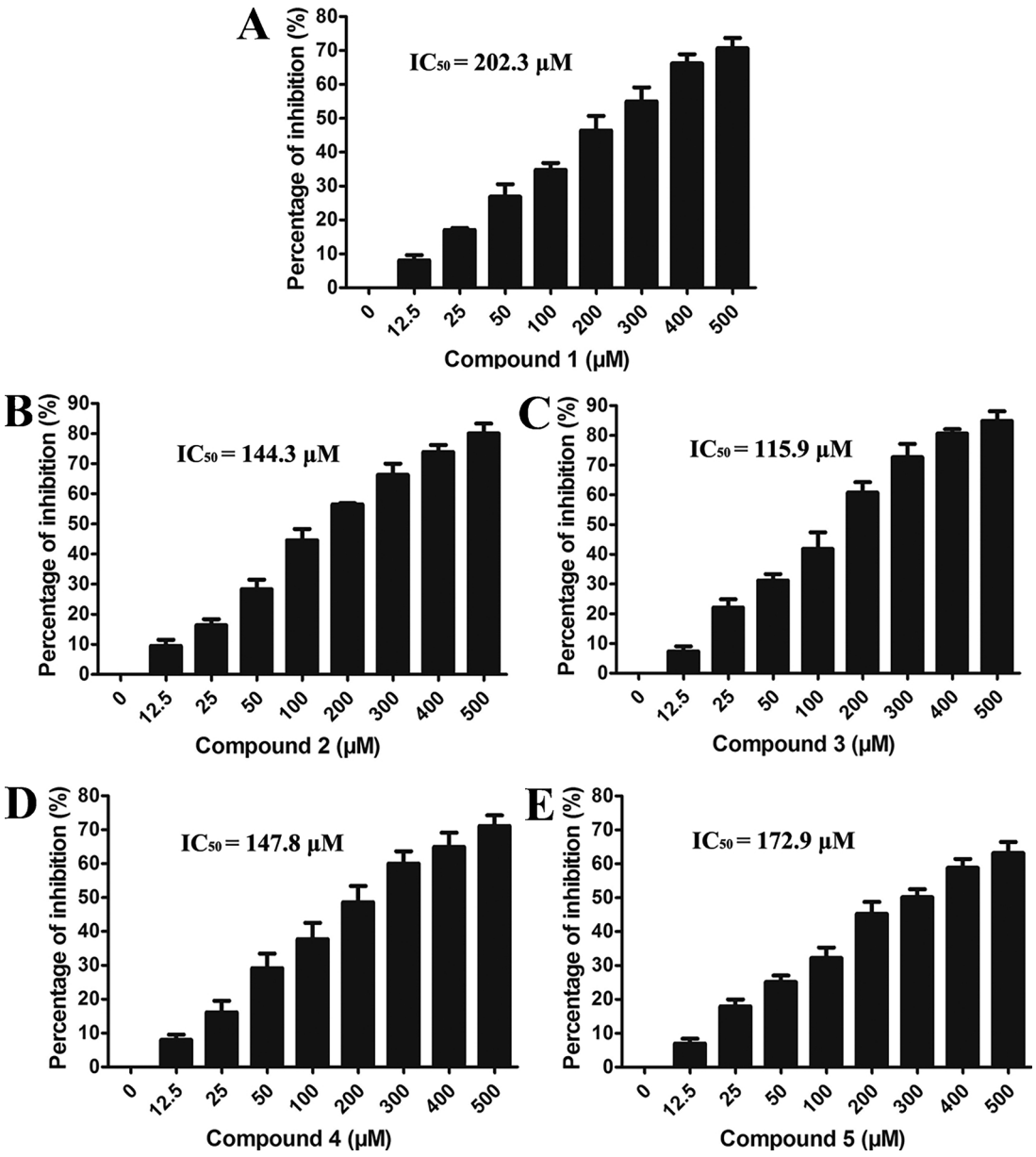

Fig. 2. Effects of compounds 1–5 on the activity of PRRSV 3CLSP in a FRET assay. Enzymatic activity was measured using substrate at 1 μM and compounds 1–5 at various concentrations (12.5–500 μM). Percentage of inhibition (%) = 100 × [1 − RFU of the experimental group (60 min–0 min)/RFU of the control group (60 min–0 min)]. IC_{50} was determined using GraphPad Prism software 5. Bars represent the SD from three replicates.

3CL protease, the S1 specificity pocket is essential for recognition of the side chain of the substrate P1 residue and determination of the enzyme's preference (Tian et al., 2009; Ye et al., 2016). Hence, the residues of S1 specificity pockets were selected as targets for molecule docking. A total of 256 binding conformations between the ligands and the proteins were obtained, and the lowest energy conformations were used for further analysis. As shown in Fig. 5A and B, compounds 2 and 3 are illustrated as sticks, and the amino acid residues contacting the compounds are shown as lines. Because there is a significant difference in the residues of S1 specificity pockets between PRRSV nsp4 and PEDV nsp5, compounds 2 and 3 were docked into 3CLSP and 3CL protease with different conformations and interactions (Fig. 5A and B). Besides, due to the semi-flexible docking was performed, the binding conformations of compounds 2 and 3 with 3CLSP or 3CL protease also exists subtle differences. Nonetheless, their interactions are highly similar (Fig. 5A and B). Otherwise, previous studies have shown that the substrate-binding sites and active sites of the 3CLSP and 3CL protease are located between domains I and II in their structures (Tian et al., 2009; Ye et al., 2016). The amino acid residue His39 in 3CLSP (corresponding to His41 of 3CL protease) plays a vital role in substrate combination and catalysis. Indeed, our docking analysis results suggested that compounds 2 and 3 bind in the substrate channel between domains I and II, which form strongly hydrophobic interactions and hydrogen bonds with His39 (or His41) (Fig. 5A). Hence, compounds 2 and 3 would be broad competitive inhibitors and bind in the substrate-binding channel of the 3CLSP and 3CL protease, replacing the substrate.

Additionally, our results showed that compounds 2 and 3 could effectively inhibit the replication of PRRSV and PEDV at a micromolar range. Unfortunately, their EC_{50} values were high (> 50 μM), and the selectivity index (SI) values were less than 10 (Figs. 3 and 4; Table 1). As lead compounds, compounds 2 and 3 have a low molecular weight (< 250 Da) (Table S1). Thus, further medicinal chemistry optimization is available to increase the selectivity index and pharmacokinetic properties (DMPK). Moreover, the substrate-binding channel of the 3CLSP or 3CL protease is a large cavity, supplementary studies may need to more accurately characterize the compound-binding sites to

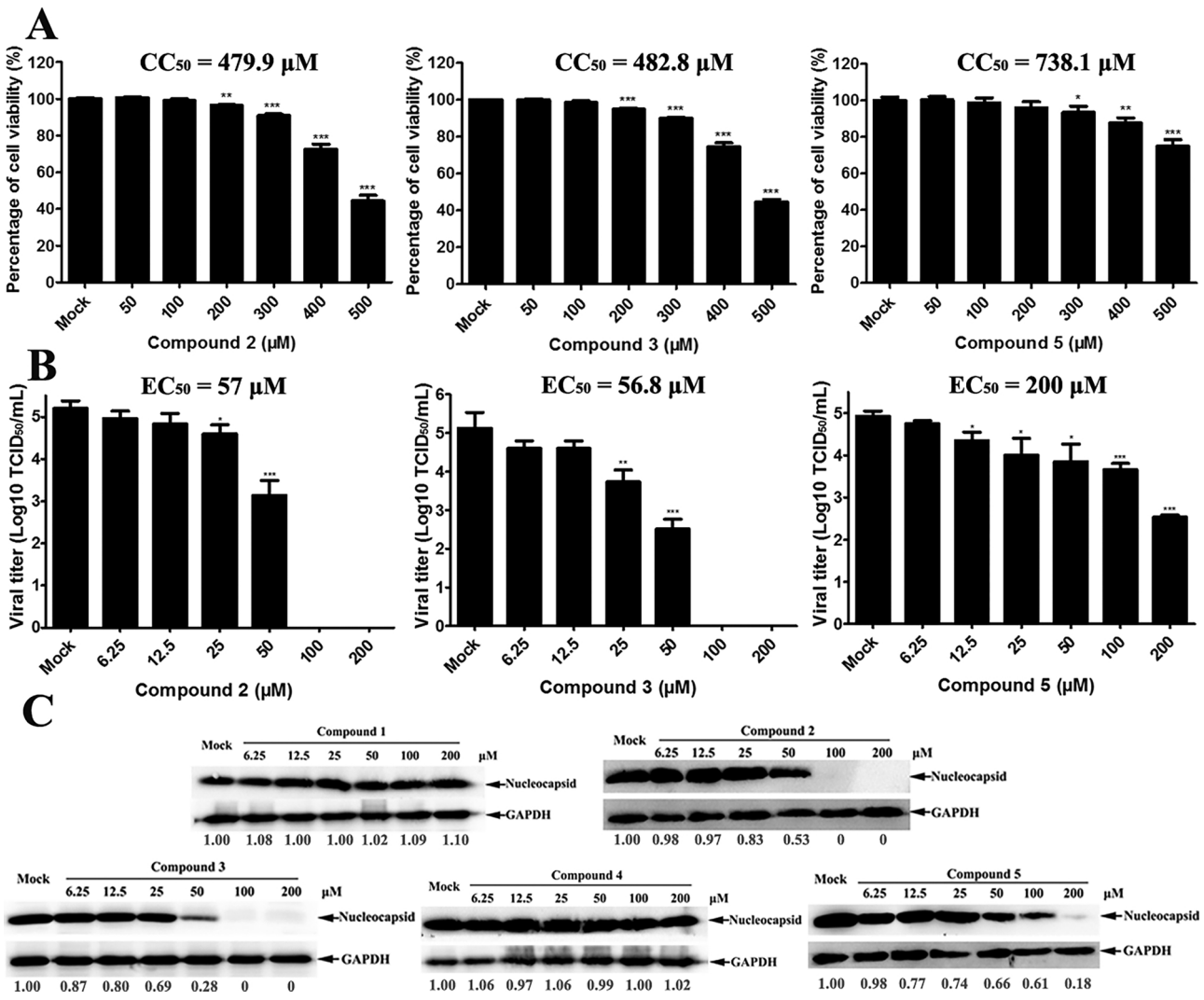

Fig. 3. Effects of compounds 2, 3 and 5 on PRRSV replication in MARC-145 cells. (A) Cell viability analysis of compounds 2, 3 and 5 (50–500 μM) in MARC-145 cells. (B) Compounds 2 and 3 inhibit PRRSV replication in MARC-145 cells. PRRSV was added with increasing concentrations of compounds (6.25 μM, 12.5 μM, 25 μM, 50 μM, 100 μM and 200 μM) at an MOI of 0.1, and then infected MARC-145 cells for 36 h. Then, the harvested supernatant (include PRRSV and compounds) was used for $TCID_{50}$ assays. (C) Dose-dependent inhibition of PRRSV nucleocapsid protein production by compounds 2, 3 and 5. MARC-145 cells were treated with 0.4% DMSO as a control, and GAPDH was loaded as an internal control. Meanwhile, PRRSV N protein levels were normalized to GAPDH. CC_{50} and EC_{50} were determined using GraphPad Prism software 5. Bars represent the SD from three replicates. *, $P < 0.05$ (considered significant compared with control group); **, $P < 0.01$ (considered highly significant); ***, $P < 0.001$ (considered extremely significant).

design and optimize inhibitors. For Norwalk virus and feline coronavirus, the transition state 3C-like protease inhibitors were designed and synthesized, and exhibited notable inhibitory effects against viral replication (Tiew et al., 2011; Kim et al., 2013). Therefore, transition state compounds that will optimally generate hydrophobic interactions and hydrogen bonds with the side chain amino acid residues are needed, and animal studies should also be conducted to develop antiviral drugs against PRRSV and PEDV in the future. Finally, our results emphasize the feasibility of developing anti-PRRSV and anti-PEDV inhibitors as a new class of broad-spectrum antiviral drugs as a treatment for exposure to viral agents.

5. Conclusions

The emerging, highly virulent PRRSV and PEDV strains have been widespread and prevalent worldwide, and seriously affect and constrain the development of the pig farming industry. In this study, we identified novel antiviral inhibitors that target PRRSV nsp4 (3CLSP), which were designated compounds 2 and 3. These two compounds could substantially inhibit PRRSV replication. Moreover, compounds 2 and 3 exhibited broad-spectrum antiviral activities, which target the PEDV 3CL protease and inhibit PEDV replication. Our results will help to guide the development of new broad-spectrum antiviral drugs against PRRSV and PEDV.

Conflict of interest statement

The authors have declared that no conflict of interest exists.

Acknowledgements

We thank Prof. Dengguo wei for discussion and data analysis of the homology modeling.

This work was supported by the National Key Basic Research and Development Program of China (Grant No. 2014CB542700), the National Natural Science Foundation of China (Grant No. 31702249 and 31722056), the Natural Science Foundation of Hubei Province of China (Grant No. 2016CFA069) and the China Postdoctoral Science Foundation (grant No.2017M612484).

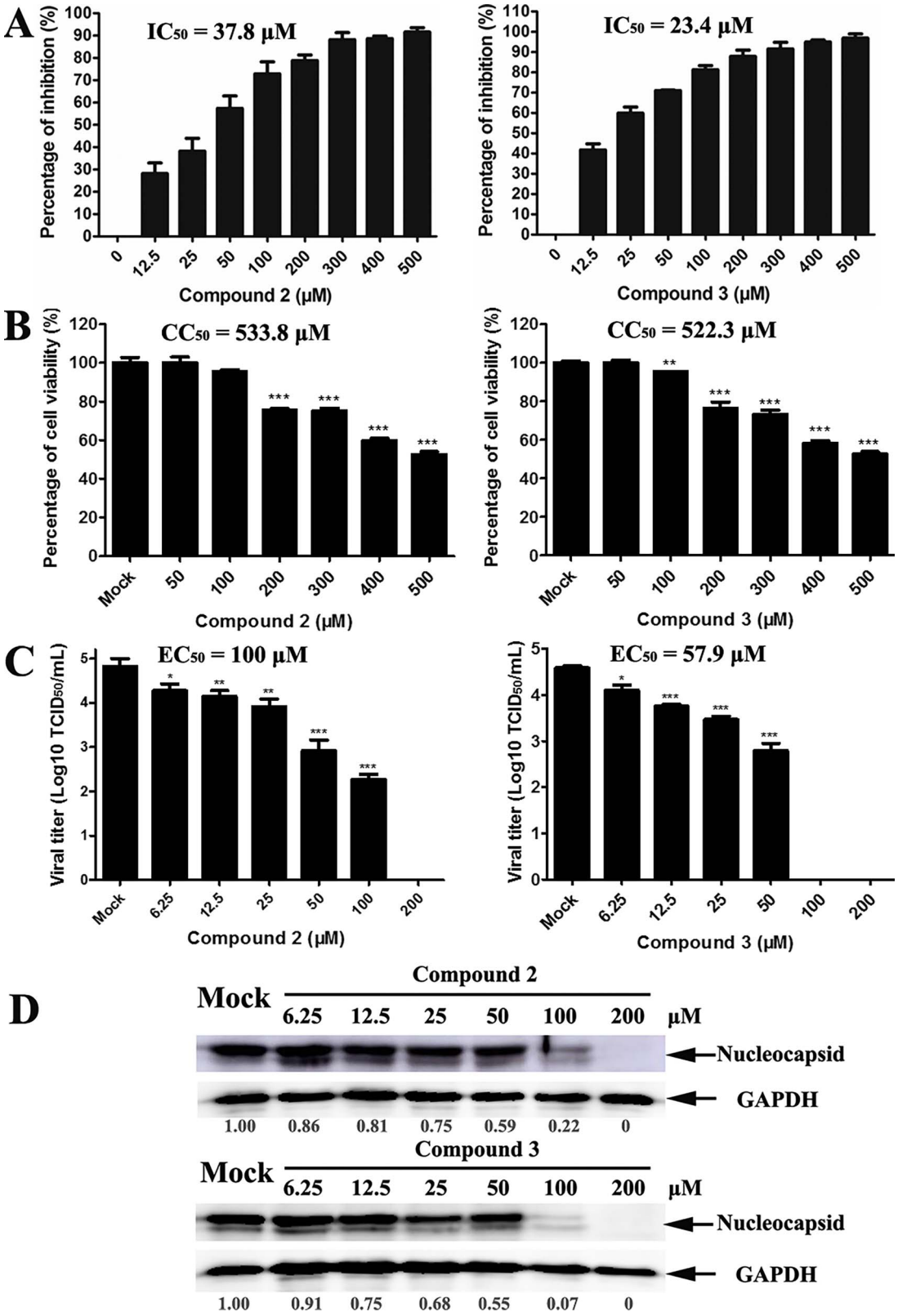

Fig. 4. Broad-spectrum inhibition of compounds 2 and 3 against PEDV. (A) Effects of compounds 2 and 3 on the 3CL protease activity of PEDV in a FRET assay. Compounds at various concentrations (12.5–500 μM) were pre-incubated with protease for 20 min at 37 ˚C, and the fluorescence values was measured. Percentage of inhibition was calculated as in Fig. 2. (B) Cell viability analysis of compounds 2 and 3 (50–500 μM) in Vero cells. (C) Compounds 2 and 3 inhibit PEDV replication in Vero cells. $TCID_{50}$ assay for PEDV was performed as in Fig. 3B. (D) Dose-dependent inhibition of PEDV nucleocapsid protein production by compounds 2 and 3. Vero cells were treated with 0.4% DMSO as a control, and GAPDH was loaded as an internal control. Meanwhile, PEDV N protein levels were normalized to GAPDH. IC_{50}, CC_{50} and EC_{50} were determined using GraphPad Prism software 5. Bars represent the SD from three replicates. *, $P < 0.05$ (considered significant compared with control group); **, $P < 0.01$ (considered highly significant); ***, $P < 0.001$ (considered extremely significant).

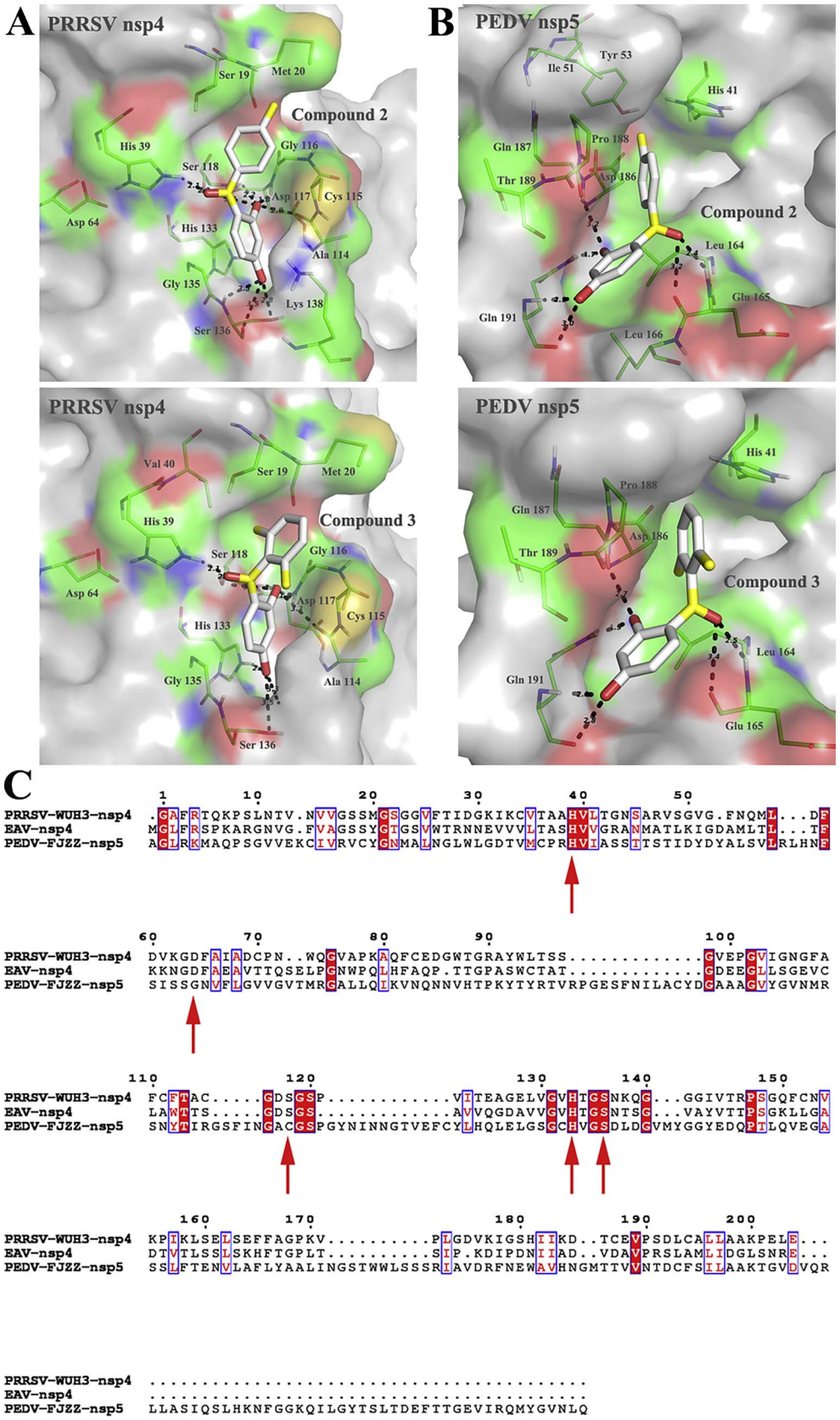

Fig. 5. Docking of compounds 2 and 3 with PRRSV 3CLSP (nsp4) and PEDV 3CL protease (nsp5). (A) Docked conformations of compounds 2 and 3 with PRRSV nsp4. The compounds and amino acid residues contacting the compounds are represented as sticks and lines, respectively (the protease surface transparency is set at 40%). The amino acid residues are colored according to atom type. Moreover, hydrogen bond interactions are shown as black dashed lines between the respective donor and acceptor atoms, along with the bond distance. (B) Docked conformations of compounds 2 and 3 with PEDV nsp5. The compounds and molecular interactions are represented as in A. (C) Sequence relationships between arterivirus 3CLSP and coronavirus 3CL protease. The amino acid sequence of EAV (GenBank: X53459.3) nsp4 was used for sequence relationship analysis. The residue numbers at the top refer to the PRRSV 3CLSP amino acid sequence. The key residues for potential 3CLSP activity sites and substrate binding sites on PRRSV are marked with red arrows at the bottom. The sequences were aligned using ClustalW2, and the alignment was drawn with ESPript 3.0. (For interpretation of the references to color in this figure legend, the reader is referred to the web version of this article.)

Appendix A. Supplementary data

Supplementary data associated with this article can be found, in the online version, at https://doi.org/10.1016/j.vetmic.2017.11.031.

References

Anand, K., Palm, G.J., Mesters, J.R., Siddell, S.G., Ziebuhr, J., Hilgenfeld, R., 2002. Structure of coronavirus main proteinase reveals combination of a chymotrypsin fold with an extra alpha-helical domain. EMBO J. 21 (13), 3213–3224.

Collins, J.E., Benfield, D.A., Christianson, W.T., Harris, L., Hennings, J.C., Shaw, D.P., Goyal, S.M., McCullough, S., Morrison, R.B., Joo, H.S., et al., 1992. Isolation of swine infertility and respiratory syndrome virus (isolate ATCC VR-2332) in North America and experimental reproduction of the disease in gnotobiotic pigs. J. Vet. Diagn. Invest. 4 (2), 117–126.
Congreve, M., Carr, R., Murray, C., Jhoti, H., 2003. A 'rule of three' for fragment-based lead discovery? Drug Discov. Today 8, 876–877.
de Kloe, G.E., Bailey, D., Leurs, R., de Esch, I.J., 2009. Transforming fragments into candidates: small becomes big in medicinal chemistry. Drug Discov. Today 14 (13–14), 630–646.
Du, L., Li, B., Pang, F., Yu, Z., Xu, X., Fan, B., Tan, Y., He, K., Huang, K., 2017a. Porcine GPX1 enhances GP5-based DNA vaccination against porcine reproductive and respiratory syndrome virus. Vet. Immunol. Immunopathol. 183, 31–39.
Du, L., Pang, F., Yu, Z., Xu, X., Fan, B., Huang, K., He, K., Li, B., 2017b. Assessment of the efficacy of two novel DNA vaccine formulations against highly pathogenic porcine reproductive and respiratory syndrome virus. Sci. Rep. 7, 41886.
Evans, A.B., Dong, P., Loyd, H., Zhang, J., Kraus, G.A., Carpenter, S., 2017. Identification and characterization of small molecule inhibitors of porcine reproductive and respiratory syndrome virus. Antiviral Res. 146, 28–35.
Gorbalenya, A.E., Enjuanes, L., Ziebuhr, J., Snijder, E.J., 2006. Nidovirales: evolving the largest RNA virus genome. Virus Res. 117 (1), 17–37.
Han, J., Zhou, L., Ge, X., Guo, X., Yang, H., 2017. Pathogenesis and control of the Chinese highly pathogenic porcine reproductive and respiratory syndrome virus. Vet. Microbiol. 209, 30–47.
Karuppannan, A.K., Wu, K.X., Qiang, J., Chu, J.J., Kwang, J., 2012. Natural compounds inhibiting the replication of Porcine reproductive and respiratory syndrome virus. Antiviral Res. 94 (2), 188–194.
Kim, H.S., Kwang, J., Yoon, I.J., Joo, H.S., Frey, M.L., 1993. Enhanced replication of porcine reproductive and respiratory syndrome (PRRS) virus in a homogeneous subpopulation of MA-104 cell line. Arch. Virol. 133 (3–4), 477–483.
Kim, Y., Mandadapu, S.R., Groutas, W.C., Chang, K.O., 2013. Potent inhibition of feline coronaviruses with peptidyl compounds targeting coronavirus 3C-like protease. Antiviral Res. 97, 161–168.
Kumar, V., Shin, J.S., Shie, J.J., Ku, K.B., Kim, C., Go, Y.Y., Huang, K.F., Kim, M., Liang, P.H., 2017. Identification and evaluation of potent Middle East respiratory syndrome coronavirus (MERS-CoV) 3CLPro inhibitors. Antiviral Res. 141, 101–106.
Larkin, M.A., Blackshields, G., Brown, N.P., Chenna, R., McGettigan, P.A., McWilliam, H., Valentin, F., Wallace, I.M., Wilm, A., Lopez, R., Thompson, J.D., Gibson, T.J., Higgins, D.G., 2007. Clustal W and Clustal X version 2.0. Bioinformatics 23 (21), 2947–2948.
Lee, C.C., Kuo, C.J., Hsu, M.F., Liang, P.H., Fang, J.M., Shie, J.J., Wang, A.H., 2007. Structural basis of mercury- and zinc-conjugated complexes as SARS-CoV 3C-like protease inhibitors. FEBS Lett. 581, 5454–5458.
Li, B., Xiao, S., Wang, Y., Xu, S., Jiang, Y., Chen, H., Fang, L., 2009. Immunogenicity of the highly pathogenic porcine reproductive and respiratory syndrome virus GP5 protein encoded by a synthetic ORF5 gene. Vaccine 27 (13), 1957–1963.
Li, W., Li, H., Liu, Y., Pan, Y., Deng, F., Song, Y., Tang, X., He, Q., 2012. New variants of porcine epidemic diarrhea virus, China, 2011. Emerg. Infect. Dis. 18 (8), 1350–1353.
Nienaber, V.L., Breddam, K., Birktoft, J.J., 1993. A glutamic acid specific serine protease utilizes a novel histidine triad in substrate binding. Biochemistry 32 (43), 11469–11475.
Robert, X., Gouet, P., 2014. Deciphering key features in protein structures with the new ENDscript server. Nucleic Acids Res. 42, W320–W324 (Web Server issue).
Shi, Y., Li, Y., Lei, Y., Ye, G., Shen, Z., Sun, L., Luo, R., Wang, D., Fu, Z.F., Xiao, S., Peng, G., 2016. A dimerization-dependent mechanism drives the endoribonuclease function of porcine reproductive and respiratory syndrome virus nsp11. J. Virol. 90 (9), 4579–4592.
Snijder, E.J., Kikkert, M., Fang, Y., 2013. Arterivirus molecular biology and pathogenesis. J. Gen. Virol. 94 (Pt 10), 2141–2163.
Song, D., Park, B., 2012. Porcine epidemic diarrhoea virus: a comprehensive review of molecular epidemiology, diagnosis, and vaccines. Virus Genes 44 (2), 167–175.
St John, S.E., Anson, B.J., Mesecar, A.D., 2016. X-Ray structure and inhibition of 3C-like protease from porcine epidemic diarrhea virus. Sci. Rep. 6, 25961.
Tian, K., Yu, X., Zhao, T., Feng, Y., Cao, Z., Wang, C., Hu, Y., Chen, X., Hu, D., Tian, X., Liu, D., Zhang, S., Deng, X., Ding, Y., Yang, L., Zhang, Y., Xiao, H., Qiao, M., Wang, B., Hou, L., Wang, X., Yang, X., Kang, L., Sun, M., Jin, P., Wang, S., Kitamura, Y., Yan, J., Gao, G.F., 2007. Emergence of fatal PRRSV variants: unparalleled outbreaks of atypical PRRS in China and molecular dissection of the unique hallmark. PLoS One 2 (6), e526.
Tian, X., Lu, G., Gao, F., Peng, H., Feng, Y., Ma, G., Bartlam, M., Tian, K., Yan, J., Hilgenfeld, R., Gao, G.F., 2009. Structure and cleavage specificity of the chymotrypsin-like serine protease (3CLSP/nsp4) of Porcine Reproductive and Respiratory Syndrome Virus (PRRSV). J. Mol. Biol. 392 (4), 977–993.
Tian, P.F., Jin, Y.L., Xing, G., Qv, L.L., Huang, Y.W., Zhou, J.Y., 2014. Evidence of recombinant strains of porcine epidemic diarrhea virus, United States, 2013. Emerg. Infect. Dis. 20 (10), 1735–1738.
Tiew, K.C., He, G., Aravapalli, S., Mandadapu, S.R., Gunnam, M.R., Alliston, K.R., Lushington, G.H., Kim, Y., Chang, K.O., Groutas, W.C., 2011. Design, synthesis, and evaluation of inhibitors of Norwalk virus 3C protease. Bioorg. Med. Chem. Lett. 21, 5315–5319.
Wang, X.M., Niu, B.B., Yan, H., Gao, D.S., Yang, X., Chen, L., Chang, H.T., Zhao, J., Wang, C.Q., 2013. Genetic properties of endemic Chinese porcine epidemic diarrhea virus strains isolated since 2010. Arch. Virol. 158 (12), 2487–2494.
Wang, D., Fang, L., Xiao, S., 2016. Porcine epidemic diarrhea in China. Virus Res. 226, 7–13.
Wei, D., Jiang, X., Zhou, L., Chen, J., Chen, Z., He, C., Yang, K., Liu, Y., Pei, J., Lai, L., 2008. Discovery of multitarget inhibitors by combining molecular docking with common pharmacophore matching. J. Med. Chem. 51, 7882–7888.
Wensvoort, G., Terpstra, C., Pol, J.M., ter Laak, E.A., Bloemraad, M., de Kluyver, E.P., Kragten, C., van Buiten, L., den Besten, A., Wagenaar, F., et al., 1991. Mystery swine disease in The Netherlands: the isolation of Lelystad virus. Vet. Q. 13 (3), 121–130.
Xuan, H., Xing, D.K., Wang, D.Y., Zhu, W.Z., Zhao, F.Y., Gong, H.J., Fei, S.G., 1984. Study on the culture of porcine epidemic diarrhea virus adapted to fetal porcine intestine primary cell monolayer. Chin. J. Vet. Sci. 4 (3), 202–208 (in Chinese).
Xue, X., Yu, H., Yang, H., Xue, F., Wu, Z., Shen, W., Li, J., Zhou, Z., Ding, Y., Zhao, Q., Zhang, X.C., Liao, M., Bartlam, M., Rao, Z., 2008. Structures of two coronavirus main proteases: implications for substrate binding and antiviral drug design. J. Virol. 82 (5), 2515–2527.
Ye, G., Deng, F., Shen, Z., Luo, R., Zhao, L., Xiao, S., Fu, Z.F., Peng, G., 2016. Structural basis for the dimerization and substrate recognition specificity of porcine epidemic diarrhea virus 3C-like protease. Virology 494, 225–235.
Ziebuhr, J., Snijder, E.J., Gorbalenya, A.E., 2000. Virus-encoded proteinases and proteolytic processing in the Nidovirales. J. Gen. Virol. 81, 853–879.